



Full paper/Mémoire

Highly selective oxidation of alcohols using $\text{MnO}_2/\text{TiO}_2\text{-ZrO}_2$ as a novel heterogeneous catalyst

Ahmad Reza Massah^{a,*,b}, Roozbeh Javad Kalbasi^{a,*,b}, Mohammad Azadi^{a,c}^a Department of Chemistry, Shahreza Branch, Islamic Azad University, 311-86145 Shahreza, Isfahan, Iran^b Razi Chemistry Research Center, Shahreza Branch, Islamic Azad University, Shahreza, Isfahan, Iran^c Young Researchers Club, Shahreza Branch, Islamic Azad University, Shahreza, Isfahan, Iran

ARTICLE INFO

Article history:

Received 6 December 2010

Accepted after revision 5 March 2012

Available online 4 April 2012

Keywords:

 MnO_2 $\text{TiO}_2\text{-ZrO}_2$

Heterogeneous catalyst

Oxidation

Benzyl alcohols

ABSTRACT

$\text{MnO}_2/\text{TiO}_2\text{-ZrO}_2$, which was synthesized by the adsorption method, demonstrated very high catalytic activity in the selective oxidation of benzyl alcohols to benzaldehydes with excellent yields and selectivity in short reaction times. The physical and chemical properties of $\text{MnO}_2/\text{TiO}_2\text{-ZrO}_2$ were investigated by XRD, XRF, BET, FT-IR and SEM techniques. The influence of the catalyst support (SBA-15, ZSM-5, $\text{TiO}_2\text{-ZrO}_2$ and Y), type of metal oxide supported, method of loading and amount of manganese nitrate loading have been thoroughly investigated. Moreover, the catalyst has shown excellent reusability in the process.

© 2012 Académie des sciences. Published by Elsevier Masson SAS. All rights reserved.

1. Introduction

The selective oxidation of alcohols to the corresponding carbonyl compounds is one of the most vital functional group transformations in organic synthesis and is extensively used in fine chemistry and pharmaceutical industries. In recent years, the development of new environmentally friendly methods for the selective oxidation of alcohols to aldehydes and ketones has attracted much attention both in industrial processes and inorganic synthesis [1]. Traditional methods for alcohol oxidation involve the use of non-catalytic system with stoichiometric amounts of oxidants, such as PCC, MnO_2 , $\text{Na}_2\text{Cr}_2\text{O}_7$, NaClO , KMnO_4 and so on [2]. These methods produce toxic by-products and large amounts of heavy metal wastes [3]. Recently, some new methods were developed for the oxidation of alcohols using heterogeneous catalyst which would overcome these disadvantages and provide a

commercial process having easy handling of the catalyst, atom utility, and possible regeneration and re-use of the catalyst [4–11].

Nanoscale metal (oxide) particles are of considerable scientific interest, e.g., they hold the potential for very efficient utilization as catalysts. Such catalysts are characterized by extremely high surface-to-volume ratios of the active species, which contributes to maximized material efficiency. Furthermore, highly dispersed metal (oxide) nanoclusters are believed to act as more active and selective catalysts than the respective bulk materials [12]. In addition, due to their high surface energies, small particles tend to aggregate easily and lose the specific characteristics which are associated with the colloidal state [12,13]. One approach to overcome this disadvantage is to stabilize particulate materials by immobilizing on suitable support materials. Mesoporous materials offer high internal surface areas. In addition, space confinement of their pores prevents the particles from growing larger than the pore size [12–14]. Recently, meso-structured oxides and mixed oxides have received considerable attention. Some of the interesting materials already tested are MCM-41, Al-MCM-41, HMS, Al-HMS, Ti-HMS, SBA-15

* Corresponding authors.

E-mail addresses: massahar@iaush.ac.ir, massahar@yahoo.com (A.R. Massah), rkalbasi@gmail.com (R.J. Kalbasi).

as supports. Although the structural stability of these materials at present is less than desirable, there are promising reports in literature to improve their stability. The fact that all these materials, which seemed promising such as $\text{ZrO}_2\text{-TiO}_2$ and $\text{TiO}_2\text{-Al}_2\text{O}_3$, can in principle be synthesized in mesoporous form with very high surface areas and hopefully, in thermally stable form, assures plenty of challenging topics of research area based on these materials in future [15].

We have previously studied several industrially important organic transformations and rearrangements using mixed metal oxides [16–18]. Thus, in order to keep conducting research on mixed oxides, in this study, we present synthesis and characterization of $\text{MnO}_2/\text{TiO}_2\text{-ZrO}_2$ as a heterogeneous catalyst for oxidation of alcohols.

2. Experimental

2.1. Materials

The chemicals used in this work include: zirconium (IV) isopropoxide (70 wt.% solution in 2-propanol, Acros), titanium(IV) *n*-butoxide (99%, Acros), cetyl pyridinium bromide (Fluka), *n*-butanol (Merck), manganese(II) nitrate tetrahydrate (Merck), Iron(III) nitrate nonahydrate (Merck), Nickel(II) nitrate hexahydrate (Merck), Cobalt(II) nitrate hexahydrate (Merck), Zinc nitrate tetrahydrate (Merck), benzoyl peroxide (Merck) were used as the precursors. All the solvents were purchased from Merck.

2.2. Synthesis of $\text{TiO}_2\text{-ZrO}_2$ mixed oxide

$\text{ZrO}_2\text{-TiO}_2$ was used as the support. This support was prepared by the sol-gel method as was described in our previous work [16]. Zirconium(IV)isopropoxide (70 wt.% solution in 2-propanol) and titanium(IV)*n*-butoxide (99%) were used as the precursors, and 2,4-pentandione (H-acac) as the complexing agent [19,20]. Appropriate amounts of zirconium propoxide and titanium *n*-butoxide were dissolved in the solvent, *n*-butanol. The solution was heated to 60 °C and the components were thoroughly mixed. Then the solution was cooled down to room temperature, and H-acac as the complexing agent was added. This clear solution was hydrolyzed with deionized water containing cetyl pyridinium bromide (CPB) surfactant (mol of surfactant/mol of alkoxide = 0.1). The solution was left overnight to hydrolyze the alkoxides, yielding transparent gels, which were dried at 110 °C to remove water and solvent, and then calcined at 500 °C for 5 h to remove the organics. The physico-chemical characterization of the support is reported in our previous works [18].

2.3. Preparation of various metal oxides supported on $\text{TiO}_2\text{-ZrO}_2$

The MnO_2 , FeO, NiO, CoO and ZnO loaded samples were prepared by adsorption method. After the calcinations, the $\text{TiO}_2\text{-ZrO}_2$ was suspended in an aqueous solution containing metal nitrate (constant 10/1 volume/weight ratio,

solution containing 23 mmol of metal per g of $\text{TiO}_2\text{-ZrO}_2$). After 2 h of contact, the powders were recovered by filtration and then dried in air at room temperature for 48 h. The filtration was aimed at eliminating most of the no adsorbed metal oxide species. Ex situ calcination was performed in air in a muffle oven, at a rate of 5 °C/min up to 400 °C. The final temperature was maintained for 3 h before cooling down to room temperature.

2.4. Preparation of MnO_2 loaded on Zolite Y, ZSM-5 and SBA-15

MnO_2/Y , $\text{MnO}_2/\text{ZSM-5}$ and $\text{MnO}_2/\text{SBA-15}$ were prepared by loading MnO_2 on Zolite Y, ZSM-5 and SBA-15 by adsorption method as described in section 2.3.

2.5. Oxidation of alcohols; general procedure

In a typical reaction, a mixture of benzyl alcohol (2 mmol) and benzoyl peroxide (1 mmol) was added in portions to a two-necked vial containing $\text{MnO}_2/\text{TiO}_2\text{-ZrO}_2$ (0.12 g) in *n*-hexane (5 mL) and a magnetic stirring bar under air at atmospheric pressure. The vial was heated at 70 °C in a preheated oil bath. The progress of the reaction was followed by TLC or gas chromatography (GC). Upon completion, the precipitate was removed by filtration and washed with more solvent (25 mL). The filtrate was washed with 10 mL of sodium hydrogen carbonate (5%, 10 mL), brine (10 mL), and dried over MgSO_4 . Evaporation of the solvent gave a product with sufficient purity for most purposes.

2.6. Characterization of products

All of the products of these reactions are known compounds [21]. They were characterized from their IR (Nicolet 400D), ^1H NMR, ^{13}C NMR spectra (Bruker DRX-500 Avance spectrometer at 500 and 125 MHz, respectively), GC (Agilent 6820 equipped with a FID detector) and GC-MS (Agilent 6890). Most importantly, no over oxidized compounds were detected by ^1H NMR and ^{13}C NMR analysis in the crude products obtained from any of the reactions.

2.7. Characterization of catalysts

The catalysts were characterized by X-ray diffraction (Bruker D8ADVANCE, Cu K_α radiation), FT-IR spectroscopy (Nicolet 400D in KBr matrix in the range of 4000–400 cm^{-1}), BET specific surface areas and BJH pore size distribution (Series BEL SORP 18, at 77 K), thermal analyzer TG-DTA (Setaram Labsys TG (STA); in a temperature range 30–1600 °C at a heating rate of 10 °C/min in N_2 atmosphere), XRF (Bruker S₄ Pioneer) and SEM (Philips, XL30, SE detector).

3. Results and discussion

3.1. Characterization of the catalysts

Fig. 1 shows the FT-IR spectra of $\text{TiO}_2\text{-ZrO}_2$, $\text{MnO}_2/\text{TiO}_2\text{-ZrO}_2$. The FT-IR spectrum was used to identify the

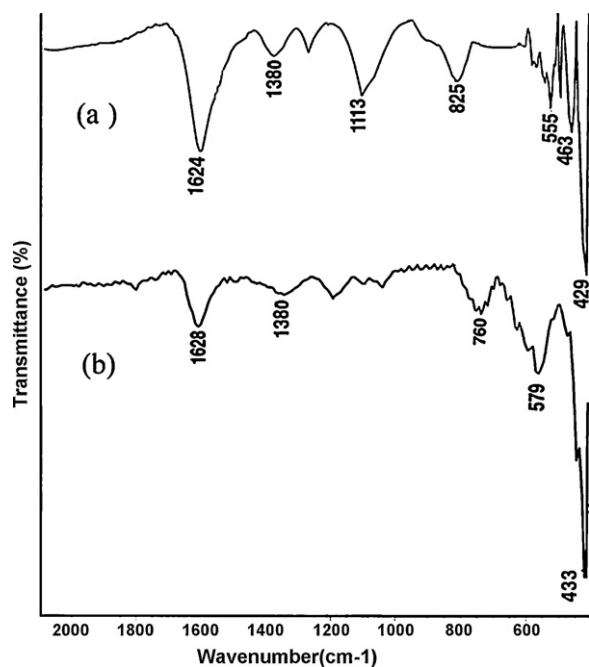


Fig. 1. The FT-IR spectra of (a) $\text{TiO}_2\text{-ZrO}_2$, (b) $\text{MnO}_2/\text{TiO}_2\text{-ZrO}_2$.

functional groups on the surface of the resulting sample. The bands around 1620 and 1380 cm^{-1} correspond to the existence of large numbers of residual hydroxyl groups, which imply the O-H vibrating mode of traces of adsorbed water. The bands located around 520 and 750 cm^{-1} can be ascribed to the Mn-O and Mn-O-Mn vibrations of MnO_2 , respectively. The FT-IR analysis presented here is consistent with the results reported in the literature [22–24]. No organic groups were found to be adsorbed on the surface on the basis of FT-IR spectra. Fig. 2 represents the FT-IR spectra of MnO_2 nano particles and $\text{MnO}_2/\text{TiO}_2\text{-ZrO}_2$ with various amounts of MnO_2 (11.5 to 46 mmol of manganese nitrate). As it can be seen from Fig. 2, the intensity of the bands located around 520 and 750 cm^{-1} increases with an increase in the amount of loaded MnO_2 on $\text{TiO}_2\text{-ZrO}_2$.

The N_2 adsorption-desorption isotherms of $\text{TiO}_2\text{-ZrO}_2$ and $\text{MnO}_2/\text{TiO}_2\text{-ZrO}_2$ samples are illustrated in Fig. 3. The isotherms are similar to the Type IV isotherm with H1-type hysteresis loops at high relative pressure according to the IUPAC classification, characteristic of mesoporous materials with highly uniform size distributions. From the two branches of adsorption-desorption isotherms, the presence of a sharp adsorption step in the P/P0 region from 0.5–0.8 and a hysteresis loop at the relative pressure P/P0 greater than 0.7 shows that the materials process a well-defined array of regular mesoporous. The specific area and the pore size have been calculated by using Brunauer-Emmett-Teller (BET) and Barrett-Joyner-Halenda (BJH) methods, respectively. The structure data of all these mesoporous materials BET surface area, total pore volume, and pore size are summarized in Table 1. It is known that calcined $\text{TiO}_2\text{-ZrO}_2$ has a high BET surface area ($270\text{ m}^2/\text{g}$), a large pore volume ($0.45\text{ cm}^3/\text{g}$) and pore size (16 nm),

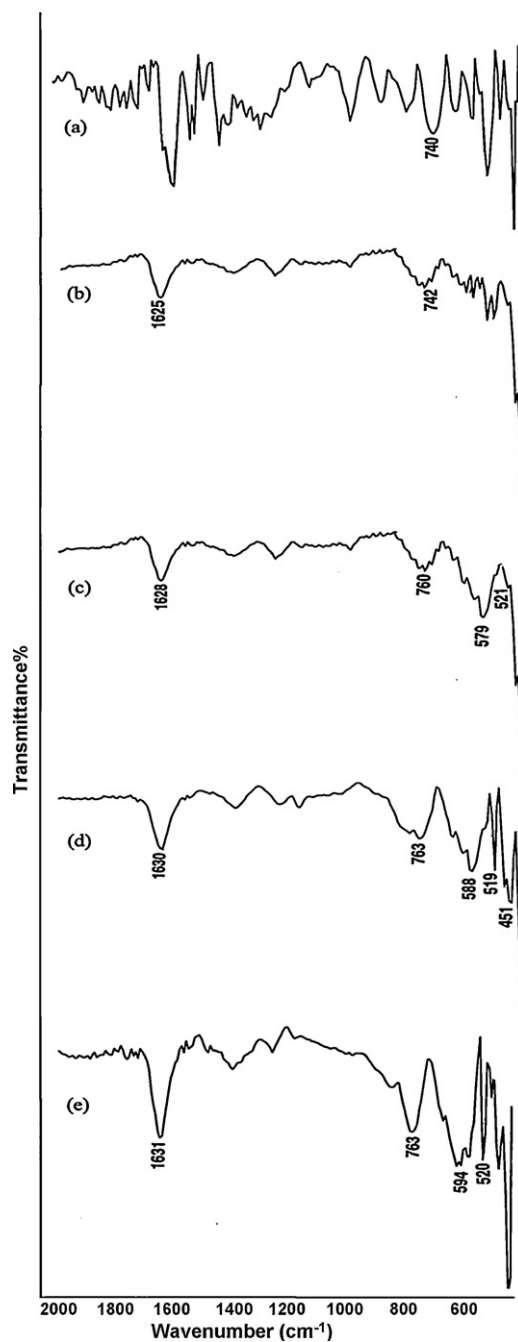


Fig. 2. The FT-IR spectra of (a) MnO_2 , (b) $\text{MnO}_2/\text{TiO}_2\text{-ZrO}_2$ (11.5 mmol of manganese nitrate), (c) $\text{MnO}_2/\text{TiO}_2\text{-ZrO}_2$ (23 mmol of manganese nitrate), (d) $\text{MnO}_2/\text{TiO}_2\text{-ZrO}_2$ (34.5 mmol of manganese nitrate) and (e) $\text{MnO}_2/\text{TiO}_2\text{-ZrO}_2$ (46 mmol of manganese nitrate).

indicative of its potential application as a host in metal oxide materials. After being modified with MnO_2 , the $\text{MnO}_2/\text{TiO}_2\text{-ZrO}_2$ exhibited smaller specific area, pore size and pore volume in comparison with those of pure $\text{TiO}_2\text{-ZrO}_2$, which might be due to the presence of MnO_2 on the pore and surface of $\text{TiO}_2\text{-ZrO}_2$ [25]. Also, XRF was performed to determine the bulk composition of catalysts

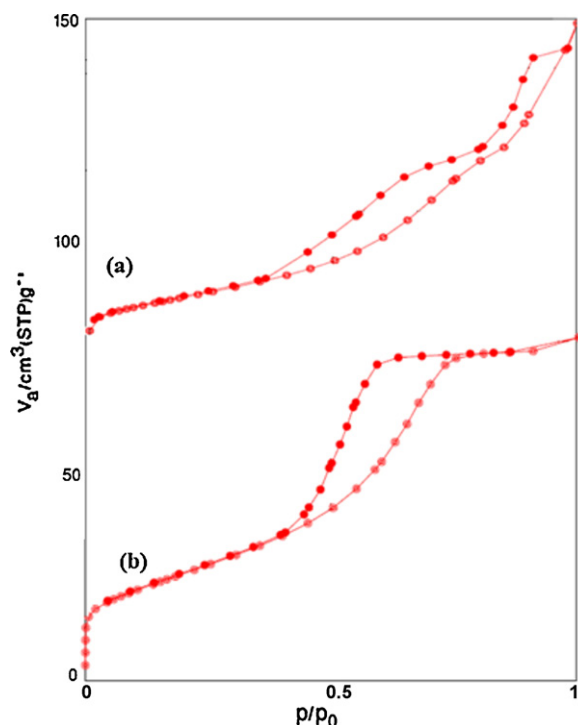


Fig. 3. Nitrogen adsorption isotherm at 77 K: (a) $\text{TiO}_2\text{-ZrO}_2$, (b) $\text{MnO}_2/\text{TiO}_2\text{-ZrO}_2$.

(Table 2). These results show that 4.167% of MnO_2 was loaded on $\text{TiO}_2\text{-ZrO}_2$.

Mao et al. have examined the crystal structures of $\text{TiO}_2\text{-ZrO}_2$ samples calcined at different temperatures from 500 to 1000 °C [26]. Their results indicate that after calcining at 500 °C, the $\text{TiO}_2\text{-ZrO}_2$ mixed oxide is in an amorphous state. However, X-ray diffraction lines, which are characteristic of the formation of the crystalline ZrTiO_4 compound, can be observed from 600 °C and higher temperatures, whose crystallinities increase with an increase in calcination temperature. These results were consistent with those reported earlier by Daly et al. [27] and Reddy et al. [28]. On the other hand, Noguchi and

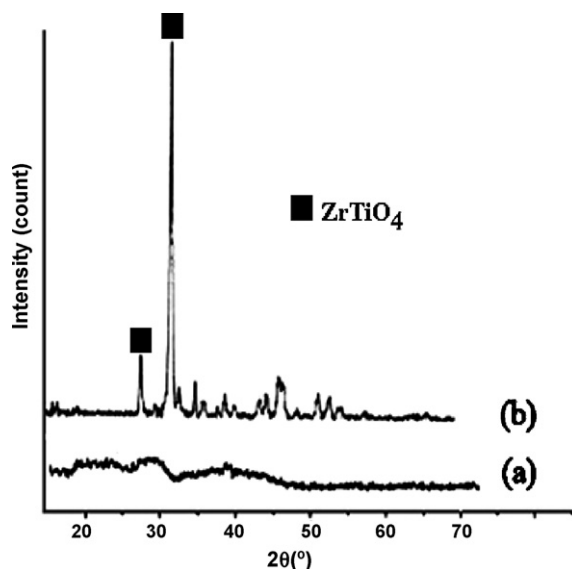


Fig. 4. The powder XRD patterns of (a) $\text{TiO}_2\text{-ZrO}_2$, (b) $\text{MnO}_2/\text{TiO}_2\text{-ZrO}_2$.

Mizuno [29] reported that tetragonal, and monoclinic ZrO_2 , and rutile TiO_2 could be produced by the decomposition of ZrTiO_4 at higher temperatures. Wu et al. [30] also found that relatively important amounts of TiO_2 (rutile) phase were separated from ZrTiO_4 at higher calcination temperatures (≥ 850 °C). Furthermore, Navio and co-workers [31] detected the formation of TiO_2 in rutile phase even after calcination at 500 °C.

The representative XRD patterns of $\text{TiO}_2\text{-ZrO}_2$ and $\text{MnO}_2/\text{TiO}_2\text{-ZrO}_2$ are depicted in Fig. 4. Crystalline ZrTiO_4 is not seen for $\text{TiO}_2\text{-ZrO}_2$ without addition of manganese nitrate after calcinations (Fig. 4a). As it is shown, when the manganese nitrate was loaded, the diffraction lines due to the formation of ZrTiO_4 compound are observed (Fig. 4b). This indicates that the transformation of amorphous $\text{TiO}_2\text{-ZrO}_2$ mixed oxide into a crystalline ZrTiO_4 compound is accelerated by the supported MnO_2 . Moreover, it was found that the intensities of these bands increase with an increase in manganese loading (Fig. 5). To the best of our knowledge, this peculiar effect of manganese oxide on the

Table 1
Porosity data of $\text{ZrO}_2\text{-TiO}_2$ and $\text{MnO}_2/\text{TiO}_2\text{-ZrO}_2$ samples.

Sample	BET surface area ($\text{m}^2 \text{g}^{-1}$)	V_p ($\text{cm}^3 \text{g}^{-1}$)	D_p (nm)
$\text{TiO}_2\text{-ZrO}_2$	270	0.45	16
$\text{MnO}_2/\text{TiO}_2\text{-ZrO}_2$	110	0.155	5.6

Table 2
Summary of composition of catalysts determined by XRF.

Catalyst	Composition of catalyst by XRF (wt%)		
	ZrO_2	TiO_2	MnO
$\text{MnO}_2/\text{TiO}_2\text{-ZrO}_2$	50.19	43.77	4.167

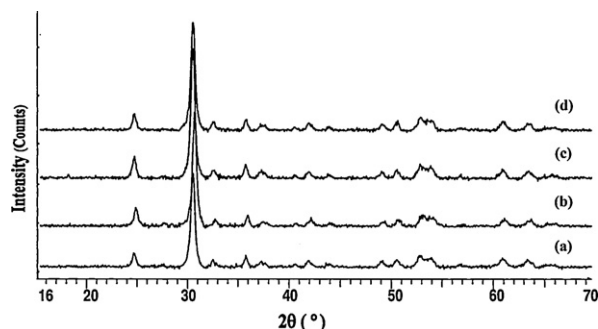


Fig. 5. The powder XRD patterns of (a) $\text{MnO}_2/\text{TiO}_2\text{-ZrO}_2$ (11.5 mmol of manganese nitrate), (b) $\text{MnO}_2/\text{TiO}_2\text{-ZrO}_2$ (23 mmol of manganese nitrate), (c) $\text{MnO}_2/\text{TiO}_2\text{-ZrO}_2$ (34.5 mmol of manganese nitrate) and (d) $\text{MnO}_2/\text{TiO}_2\text{-ZrO}_2$ (46 mmol of manganese nitrate).

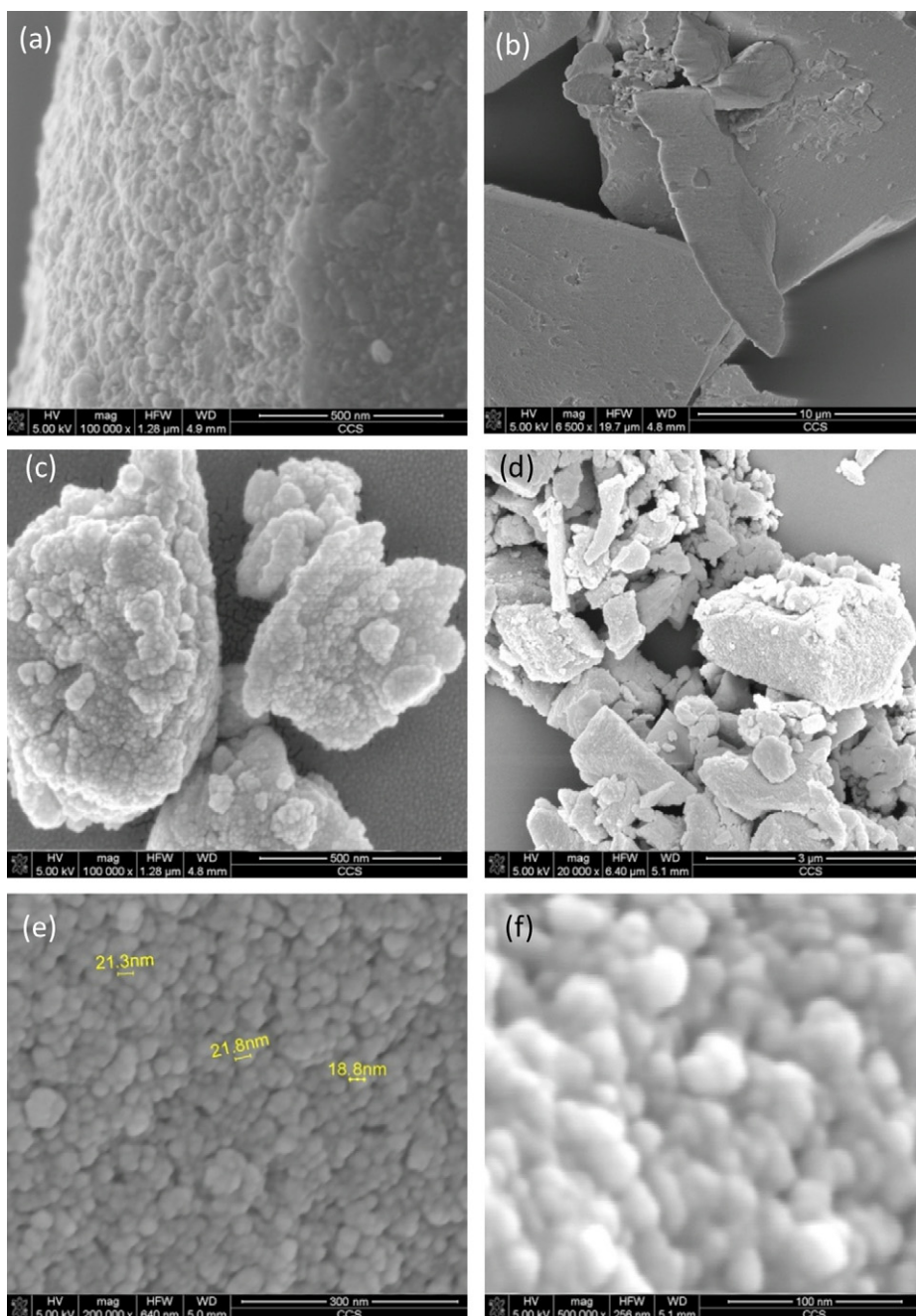


Fig. 6. SEM micrographs of samples at different magnifications: (a, b) $\text{TiO}_2\text{-ZrO}_2$, (c–f) $\text{MnO}_2/\text{TiO}_2\text{-ZrO}_2$.

crystallization of amorphous oxide has never been reported so far.

The morphology of the resulting sample was investigated by scanning electron microscopy. Fig. 6 illustrates the scanning electron microscopic (SEM) images of the $\text{TiO}_2\text{-ZrO}_2$ and $\text{MnO}_2/\text{TiO}_2\text{-ZrO}_2$. SEM images show the external morphology of the $\text{TiO}_2\text{-ZrO}_2$ which consists of spherical agglomerates with sizes of 30–70 nm (Fig. 6a, b). As can be seen, there are not huge differences between the images of the support and of the catalyst. However, it can be

seen that the $\text{TiO}_2\text{-ZrO}_2$ nanoparticles, covered (partially) with Mn oxide (Fig. 6c–f).

3.2. Catalytic activity

It is highly desirable that by supporting manganese dioxide on $\text{TiO}_2\text{-ZrO}_2$, the activity of manganese dioxide is enhanced by the additive, while the mechanical strength and thermal stability are sustained by mixed oxide. The present study appears to represent the first

Table 3
Effect of metal oxide supported in oxidation of benzyl alcohol.^a

Catalyst	Time (min)	Yield (%) ^b
TiO ₂ -ZrO ₂	10	–
MnO ₂	10	35
MnO ₂ /TiO ₂ -ZrO ₂	10	90
ZnO/TiO ₂ -ZrO ₂	10	50
CoO/TiO ₂ -ZrO ₂	10	40
NiO/TiO ₂ -ZrO ₂	10	60
FeO/TiO ₂ -ZrO ₂	10	60

^a Reaction conditions: benzyl alcohol (2 mmol), *n*-hexane (5 mL), catalyst (0.12 g), oxidant (0.25 g), T = 70 °C, loaded manganese nitrate (23 mmol), time (10 min).

^b Isolated yield.

attempt to compare the effects of titania and zirconia to supported manganese dioxide in selective oxidation of alcohols.

3.2.1. Effect of metal oxide supported

Various metal oxides supported on TiO₂-ZrO₂ were studied for selective oxidation of benzyl alcohol with benzoyl peroxide. Among cobalt, nickel, zinc, ferrum, and manganese oxides catalysts, the loaded manganese dioxide on TiO₂-ZrO₂ showed the highest yield (90%). The results are presented in Table 3. The reaction was also studied in the absence of the loaded metal oxides catalyst. No formation of benzaldehyde was observed in this case. We used MnO₂ (with the same ratio of the optimized catalyst) without any support as catalyst in the benzyl alcohol oxidation, keeping other parameters constant. After 10 min, about 35% yield was observed. It shows that TiO₂-ZrO₂ as a support is very useful for the oxidation reaction. Therefore, MnO₂/TiO₂-ZrO₂ was used for further study.

Also, the effect of Mn amount on TiO₂-ZrO₂ on the catalytic activity of MnO₂/TiO₂-ZrO₂ on the oxidation reaction of benzyl alcohol was studied. The result showed that the yield of benzaldehyde increased from 70% to 90% as the manganese nitrate loading increased from 11.5 mmol to 23 mmol. Higher amounts of manganese nitrate did not improve the yield using 0.12 g of the catalyst. Furthermore, the results showed that the yield of benzaldehyde decreased with decreasing the amounts of the catalyst from 0.12 to 0.06 g. by increasing the amount of the catalyst to 0.14 g, the yield of benzaldehyde was decreased to 70% and other oxidation by-products were observed. So, we chose 0.12 g of the catalyst as the optimized condition for further study. The reaction was also studied in the absence of the catalyst. No formation of benzaldehyde was observed in this case.

3.2.2. Effect of support on the catalytic activity

A comparison of the catalytic activity of various supports for the oxidation of benzyl alcohol to benzaldehyde is depicted in Table 4. As can be seen, the MnO₂/TiO₂-ZrO₂ catalyst shows excellent selectivity and reasonable yield for the oxidation of benzyl alcohol at 70 °C in *n*-hexane. The use of zirconium oxide as catalyst support has several advantages over other conventional oxide supports such as alumina and silica. The advantages of using zirconium as a catalyst support include: interacts

Table 4
Effect of support on the activity of catalyst.^a

Entry	Catalyst	Yield (%) ^b
1	MnO ₂ /TiO ₂ -ZrO ₂	90
2	MnO ₂ /Y	70
3	MnO ₂ /SBA-15	70
4	MnO ₂ /ZSM-5	80

^a Reaction conditions: benzyl alcohol (2 mmol), *n*-hexane (5 mL), catalyst (0.12 g), oxidant (0.25 g), T = 70 °C, loaded manganese nitrate (23 mmol), time (10 min).

^b Isolated yield.

Table 5
Oxidation of benzyl alcohol in different solvent.^a

Entry	Solvent	Yield (%) ^b
1	–	Very less
2	H ₂ O	40
3	Methanol	65
4	Acetonitrile	70
5	Toluene	80
6	<i>n</i> -hexane	90

^a Reaction conditions: benzyl alcohol (2 mmol), solvent (5 mL), catalyst (0.12 g), oxidant (0.25 g), T = 70 °C, loaded manganese nitrate (23 mmol), time (10 min).

^b Isolated yield.

strongly with the active phase; possesses high thermal stability and more chemically inert than the conventional supported oxides; it is the only metal oxide which may possess four chemical properties, namely acidity, basicity as well as the reducing and oxidizing ability. More active and stable catalysts can be obtained by incorporating transition metals, especially noble metals into the ZrO₂ system [17]. The physico-chemical characterization of TiO₂-ZrO₂ is reported in our previous works [32–34]. It is known that calcinated TiO₂-ZrO₂ has a high BET surface area (270 m²/g), a large pore volume (0.55 cm³/g) and pore size (16 nm), which is indicative of its potential application as a host in MnO₂. After being modified with MnO₂, MnO₂/TiO₂-ZrO₂ exhibited smaller specific area, pore size and pore volume in comparison with those of pure TiO₂-ZrO₂. So according the above explanation, we could expect that TiO₂-ZrO₂ is the best support for MnO₂ among other used support and MnO₂/TiO₂-ZrO₂ shows high catalytic activity.

3.2.3. Effects of solvent, oxidant and reaction temperature

The oxidation of alcohols was carried out at reflux temperature using various solvent such as water, methanol, acetonitrile, toluene, *n*-hexane and also solvent-free conditions over MnO₂/TiO₂-ZrO₂ (Table 5). The best yield of benzaldehyde was obtained when the reaction was carried out in *n*-hexane. Also, the oxidation of benzyl alcohol was examined at room temperature, 40 °C, 50 °C, 60 °C and 70 °C. The results demonstrated that the yield at 70 °C (reflux) is better than other temperatures.

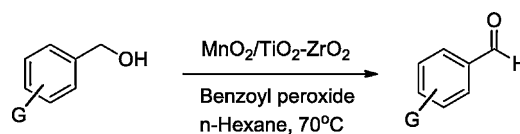
Finally, various oxidants including benzoyl peroxide, hydrogen peroxide and tert-butyl hydroperoxide were used for the oxidation of benzyl alcohols over MnO₂/TiO₂-ZrO₂. The best yield of product (90%) was obtained when benzoyl

peroxide was used as oxidant. No formation of benzaldehyde was observed in the absence of any oxidants.

3.2.4. Application of $\text{MnO}_2/\text{TiO}_2\text{-ZrO}_2$ in oxidation of various benzyl alcohols

After optimizing the reaction condition, the catalytic activity of $\text{MnO}_2/\text{TiO}_2\text{-ZrO}_2$ was investigated for the oxidation of various alcohols (Scheme 1).

Both benzyl and non-benzyl primary alcohols as well as the secondary benzyl alcohols were found to be oxidized in good to excellent yields (Table 6). Several functionalities present in the phenyl ring such as halogen, hydroxyl, methoxy, and nitro groups in various positions (*o*, *m*, *p*) were tolerated. In all cases, the corresponding aldehydes were obtained in good to excellent yields and purity. It should be mentioned that all of the reactions occurred with complete selectivity for aldehydes or ketones and no other



Scheme 1.

products were detected in the reaction mixture. Comparing the oxidation of 2-Hydroxy benzyl alcohol, having electron-donating group, (Table 6, entry 7) benzyl alcohol without group on loop (Table 6, entry 1) and 4-nitro benzyl alcohol, having electron-withdrawing group, (Table 6, entry 13) shows that oxidation of alcohols with electron-donating groups was performed faster than alcohols without groups on loop. Electron-withdrawing group

Table 6
Oxidation of aromatic aldehydes catalyzed by $\text{MnO}_2/\text{TiO}_2\text{-ZrO}_2$.^a

Entry	Alcohol	Product	Time (min)	Yield (%) ^b
1			10	90
2			20	80
3			30	70
4			20	75
5			20	70
6			30	68
7			5	95
8			5	99
9			20	60

Table 6 (Continued)

Entry	Alcohol	Product	Time (min)	Yield (%) ^b
10			50	80
11			30	70
12			40	90
13			20	50
14			40	75
15			20	90
16			40	60
17			20	85
18			30	90
19			20	55
20			20	80

^a Reaction conditions: alcohol (2 mmol), solvent (5 mL, *n*-hexane), catalyst (0.12 g), oxidant (0.25 g), T = 70 °C, loaded manganese nitrate (23 mmol).

^b Isolated yield.

decreased reaction rate and yield. Having compared 2-hydroxy benzyl alcohol and 2-methyl benzyl alcohol which both have electron donor group, we found out that the oxidation 2-hydroxy benzyl alcohol which has more powerful electron-donating group was performed faster.

3.2.5. Study of the reusability of the catalyst

In order to know whether the catalyst would succumb to poisoning and lose catalytic activity during the oxidation reaction, the solid catalyst was recovered after the reaction. The recovered catalyst from the experiment

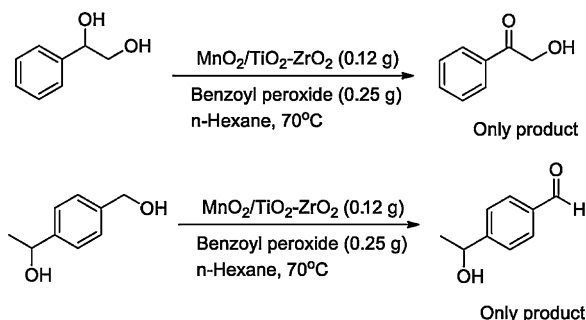
Table 7
Reusability of the catalyst.^a

Cycle	Fresh	1th	2nd	3rd
Yield (%) ^{b,c}	90	88	88	87

^a Reaction conditions: benzyl alcohol (2 mmol), solvent (5 mL, *n*-hexane), catalyst (0.12 g), oxidant (0.25 g), T = 70 °C, loaded manganese nitrate (23 mmol), time (10 min).

^b Isolated yield.

^c Catalyst was calcined at 400 °C.



was washed with water (10 mL) and acetone (3 × 5 mL), then was dried and calcined at 400 °C and used in the oxidation of benzyl alcohol. The obtained results are provided in Table 7. The results show that the catalyst can be reused four times without any modification and no significant loss of activity/selectivity performance was observed.

3.2.6. Chemoselectivity of the Catalyst

In order to examine the chemoselectivity of the present method, 1-phenylethane-1,2-diol was allowed to react with benzoyl peroxide in *n*-hexane in the presence of the MnO₂/TiO₂-ZrO₂. As depicted in Scheme 2, the catalyst was able to discriminate between benzylic and non-benzylic alcohols and showed a high chemoselectivity for oxidation of benzylic alcohols. Also, the catalyst shows discriminate between primary and secondary benzyl alcohols and exhibited a high chemoselectivity to primary benzylic alcohols.

4. Conclusion

MnO₂/TiO₂-ZrO₂ is an active and environmentally friendly catalyst for liquid phase oxidation of alcohols. With almost identical manganese dioxide loading by adsorption method, MnO₂/TiO₂-ZrO₂ exhibited better catalytic behaviors than other used catalysts. This catalyst

also showed excellent reusability in the process. Surprisingly, in the presence of this catalyst and at the optimized conditions, there were not any by-products.

Acknowledgements

The Support from Islamic Azad University, Shahreza Branch (IAUSH) Research Council and Iranian Nanotechnology Initiative Council is gratefully acknowledged.

References

- [1] R.A. Sheldon, I.W.C.E. Arends, A. Dijkman, *Catal. Today* 57 (2000) 157.
- [2] S. Zhang, S. Gao, Z. Xi, J. Xu, *Catal. Commun.* 8 (2007) 531.
- [3] R.A. Sheldon, I.W.C.E. Arends, G.T. Brink, A. Dijkman, *Acc. Chem. Res.* 35 (2002) 774.
- [4] D. Choudhary, S. Paul, R. Gupta, J.H. Clark, *Green Chem.* 8 (2006) 479.
- [5] T. Mallat, A. Baiker, *Chem. Rev.* 104 (2004) 3027.
- [6] K. Yamaguchi, N. Mizuno, *Angew. Chem. Int. Ed.* 41 (2002) 4538.
- [7] M. Islam, P. Mondal, S. Mondal, S. Mukherjee, A.S. Roy, M. Mubarak, M. Paul, *J. Inorg. Organomet. Polym.* 20 (2010) 87.
- [8] B. Monteiro, S. Gago, P. Neves, A.A. Valente, I.S. Gonçalves, C.C.L. Pereira, C.M. Silva, M. Pillinger, *Catal. Lett.* 129 (2009) 350.
- [9] V.R. Choudhary, D.K. Dumbre, V.S. Narkhede, S.K. Jana, *Catal. Lett.* 86 (2003) 229.
- [10] V.R. Choudhary, D.K. Dumbre, B.S. Uphade, V.S. Narkhede, *J. Mol. Catal. A* 215 (2004) 129.
- [11] L. Liu, J. Ma, J. Xia, L. Li, Ch. Li, X. Zhang, J. Gong, Zh. Tong, *Catal. Commun.* 12 (2011) 323.
- [12] J.D. Aiken, R.G. Finke, *J. Mol. Catal. A: Chem.* 145 (1999) 1.
- [13] A. Taguchi, F. Schüth, *Micropor. Mesopor. Mater.* 77 (2005) 1.
- [14] J.M. Thomas, R. Raja, *Chem. Rec.* 1 (2001) 448.
- [15] G. Murali Dhar, B.N. Srinivas, M.S. Rana, Manoj Kumar, S.K. Maity, *Catal. Today* 86 (2003) 45.
- [16] M. Ghiaci, R.J. Kalbasi, H. Aghaei, *Catal. Commun.* 8 (2007) 1843.
- [17] M. Ghiaci, R.J. Kalbasi, M. Mollahasani, H. Aghaei, *Appl. Catal. A: Gen.* 320 (2007) 35.
- [18] M. Ghiaci, A. Abbaspur, R.J. Kalbasi, *Appl. Catal. A: Gen.* 287 (2005) 83.
- [19] J.M. Miller, L.J. Lakshmi, *J. Phys. Chem.* 102B (1998) 6465.
- [20] J.M. Miller, D. Wails, J.S. Beletie, *J. Chem. Soc. Faraday Trans.* 94 (1998) 789.
- [21] A. Shaabani, P. Mirzaei, S. Naderi, D.G. Lee, *Tetrahedron* 60 (2004) 11415.
- [22] X.J. Yang, Y. Makia, Z.H. Liu, K. Sakane, K. Ooi, *Chem. Mater* 16 (2004) 5581.
- [23] R. Yang, Z. Wang, L. Dai, L. Chen, *Mater. Chem. Phys.* 93 (2005) 149.
- [24] S. Jana, S. Basu, S. Pande, S.K. Ghosh, T. Pal, *J. Phys. Chem. C* 111 (2007) 16272.
- [25] M. Colilla, F. Balas, M. Manzano, M. Vallet-Regí, *Chem. Mater* 19 (2007) 3099.
- [26] D.S. Mao, G.Z. Lu, Q.L. Chen, Z.K. Xie, Y.X. Zhang, *Catal. Lett.* 77 (2001) 119.
- [27] F.P. Daly, H. Ando, J.L. Schmitt, E.A. Sturm, *J. Catal.* 108 (1987) 401.
- [28] B.M. Reddy, B. Manohar, S. Mehdi, *J. Solid State Chem.* 97 (1992) 233.
- [29] T. Noguchi, M. Mizuno, *Sol. Energy* 11 (1967) 56.
- [30] J.C. Wu, C.S. Chung, C.L. Ay, I. Wang, *J. Catal.* 87 (1984) 98.
- [31] J.A. Navio, F.J. Marchena, M. Macias, P.J. Sanchez-Soto, P. Pichat, *J. Mater. Sci.* 27 (1992) 2463.
- [32] R.J. Kalbasi, A.R. Massah, Z. Barkhordari, *Bull. Korean Chem. Soc.* 31 (2010) 2361.
- [33] R.J. Kalbasi, A. Abbaspurad, A.R. Massah, F. Zamani, *Chin. J. Chem.* 28 (2010) 273.
- [34] R.J. Kalbasi, A.R. Massah, F. Zamani, H. Javaherian Naghash, *Chin. J. Chem.* 28 (2010) 397.